3rd EUROPEAN CONFERENCE ON
EARTHQUAKE ENGINEERING & SEISMOLOGY
BUCHAREST, ROMANIA, 2022

Geophysical surveys for the characterization of the seismic local response at instrumented sites: a case study from a station of the Swiss strong motion network

Paolo Bergamo – Swiss seismological Service (SED) at ETH Zurich, Switzerland (paolo.bergamo@sed.ethz.ch)

Francesco Panzera – Swiss seismological Service (SED) at ETH Zurich, Switzerland (francesco.panzera@sed.ethz.ch)

Manuel Hobiger – Swiss seismological Service (SED) at ETH Zurich, Switzerland; Federal Institute for Geosciences and Natural Resources (BGR), Hanover, Germany (manuel.hobiger@bgr.de)

Clotaire Michel - Swiss seismological Service (SED) at ETH Zurich, Switzerland; Zurich University of Applied Sciences (ZHAW), Zurich, Switzerland (clotaire.michel@zhaw.ch)

Donat Fäh - Swiss seismological Service (SED) at ETH Zurich, Switzerland (donat.faeh@sed.ethz.ch)

Abstract: Site characterization surveying is one of the key efforts for the understanding of local amplification effects in earthquake engineering. In this perspective, geophysical measurements for the estimation of the physical properties of the subsurface at instrumented sites are particularly important. For instance, the comparison between simulated site amplification based on the retrieved Vs profile and empirical local response observed at the station allows assessing whether the site is characterized by a purely 1D response or additional 2D-3D effects are present. We present a case study involving a site characterization measurement at a station of the Swiss strong-motion network. The survey includes active seismic data acquisition along two geophone lines, of 15 and 115 m length, for the imaging of the near-surface and deeper layers, respectively. The acquired data were interpreted in terms of P-wave refraction and Rayleigh-wave multi-modal propagation analysis. The reconstructed Vs-Vp profiles achieve a high level of accuracy over a wide depth range and allow modelling the SH-transfer function of the local soil column; the latter is in excellent agreement with the local amplification function estimated by means of empirical spectral modelling of the station's recordings. The agreement confirms a purely 1D site response for the surveyed station.

Keywords: Seismic site response, geophysical surveys, wavefield decomposition, strong-motion station, empirical spectral modelling

1. Introduction

In engineering seismology, determining the soil geophysical properties related to seismic amplification at instrumented sites is a key effort. Besides improving the robustness of the estimation of seismic attenuation and of earthquake magnitudes, it contributes to explaining site effects. Therefore, site characterization campaigns are systematically implemented by network operators to reconstruct the local soil condition at the station locations (e.g. Foti et al. 2011, Yong et al. 2013, Michel et al. 2014, Kaiser et al. 2017, Hollender et al. 2018, Hobiger et al. 2021). For the purposes of site characterization, surface wave (SW) methods are nowadays regarded as an established technique (e.g. Garofalo et al. 2016a, 2016b). The relevant processing techniques commonly imply the translation of the acquired data from space-time to the spectral domain, where the

dispersion and/or ellipticity curves are then identified (e.g. Mc Mechan & Yedlin 1981, Park et al. 1999, Zywicki 1999, Xia et al. 2007). Following a different approach, the wavefield decomposition technique proposed by Maranò et al. (2012) is a relatively recent development; it targets the identification of multiple surface wave modes embedded within the wavefield recorded by an array of three-component receivers, and the joint reconstruction of their propagation parameters. Originally formulated for the processing of ambient vibration data (Maranò et al., 2012), the technique has been also adapted to the processing of Rayleigh wave data from active seismic surveys (Maranò et al., 2017), with an appropriate modelling of near-source propagation features (e.g. circular wavefront, amplitude decay, near-field effects). The wavefield-decomposition technique aims at jointly estimating, with a maximum likelihood approach, the vectors θ of the propagation parameters (azimuth, phase velocity and, for Rayleigh wave only, ellipticity) of surface waves (Love and Rayleigh waves, possibly with multiple propagation modes). The wavefield-decomposition processing code, named WaveDec, can be accessed at https://stefanomarano.github.io/WaveDec/. It is worth mentioning that the Rayleigh wave ellipticity in Maranò et al. (2012) is modelled (and retrieved) as a quantity named ellipticity angle (ξ), whose absolute value is the arctangent of the ratio of the absolute spectral amplitudes on the radial and vertical components, and whose sign relates to the sense of rotation of the Rayleigh wave elliptical particle motion. For $-\pi/2 < \xi < 0$ the particle motion is retrograde, and for $0 < \xi < \pi/2$ the motion is prograde. This latter piece of information can be of key importance for the mode identification; for instance, the fundamental mode is generally characterized by a retrograde particle motion (e.g. Foti et al., 2015), although a transition to prograde motion may occur in case of a strong impedance contrast in the subsurface, and therefore be indicative of the latter (Hobiger et al., 2013).

In this work, we present a case study of geophysical surveying at a site of the Swiss strong-motion network (SSMNet). We illustrate the advantages offered by processing active Rayleigh wave data with the wavefield-decomposition approach, in particular in terms of identification and numbering of the modal curves. The Rayleigh wave analysis is coupled with a P-wave refraction survey, which allows the reconstruction of the V_P profile and assessing the presence of possible lateral variations. The S-wave velocity model is reconstructed from the inversion of Rayleigh wave data, and its accuracy over a wide depth range is evaluated. The SH-transfer modelled from the retrieved V_S model is compared with the local amplification function, estimated by means of empirical spectral modelling of the station's recordings (Edwards et al. 2013). We conclude on the role that a thorough, multi-method geophysical surveying can play in characterizing the local seismic site response and determining whether 2-3D resonance effects are present or not (e.g., Laurendeau et al., 2018, Kaklamos and Bradley, 2018. Tao and Rathje 2020).

2. Data acquisition

The case study we show is a site characterization measurement performed at the station SFEL of the Swiss Strong Motion Network (SSMNet, https://doi.org/10.12686/sed/networks/ch); the station was installed, and the ensuing survey performed, in the framework of the SSMNet renewal project (Michel et al. 2014, Bergamo et al. 2016, Hobiger et al. 2021). Station SFEL is located in northern Switzerland (Fig. 1a) close to an important research facility (Paul Scherrer Institut), about 300 m east of the right bank of the Aare river. According to the available geological information (Swisstopo, 2006), the weathering layers are constituted by fluvioglacial terrace deposits of the late

Pleistocene; these overlay the local bedrock (Swiss Molasse), which is expected at a depth of circa 50 m at the location of SFEL (Swisstopo, 2019). The thick tree coverage made the area unsuitable for the deployment of wide arrays for the recording of ambient vibrations, requiring a stable GPS connection; therefore, we opted for an active seismic survey, accompanied by a single-station noise recording for horizontal-to-vertical spectral ratio analysis (HVSR, Nakamura 1989). As for the active measurement, we successively deployed two lines of three-component, 4.5 Hz geophones. Line 2, constituted by 16 geophones spaced by 1 m, was aligned close to SFEL, aiming at investigating in detail the shallow subsurface beneath SFEL (Fig. 1b). Due to logistical constraints, line 1 (24 geophones, 5 m spacing) was arranged slightly south; with its long spread, it was intended to target the depth range at the interface between sediments and bedrock. At both lines, we performed multichannel analysis of surface waves (MASW; Park et al., 1999) and P-wave refraction (Redpath, 1973) acquisitions. As for the latter, we positioned the active source, a 6-kg sledgehammer hitting a metal plate (Fig. 2c and 2d), at the extremities of both lines, as well as at two intermediate locations of line 1 (Fig. 1b). For the MASW acquisition, the shot points were moved outside of the arrays, at an offset of 3 m (line 2) and 30 m (line 1) from the extremities of the two lines; for line 1, having to cover a maximum offset of 145 m, we replaced the sledgehammer with a 120 kg free falling mass, dropped from 1.3 m height (Fig. 2a and 2b). Fig. 1c shows a sample seismogram acquired by line 1, with the weight drop as active source; it is possible to clearly identify the Rayleigh wave train even at far offset.

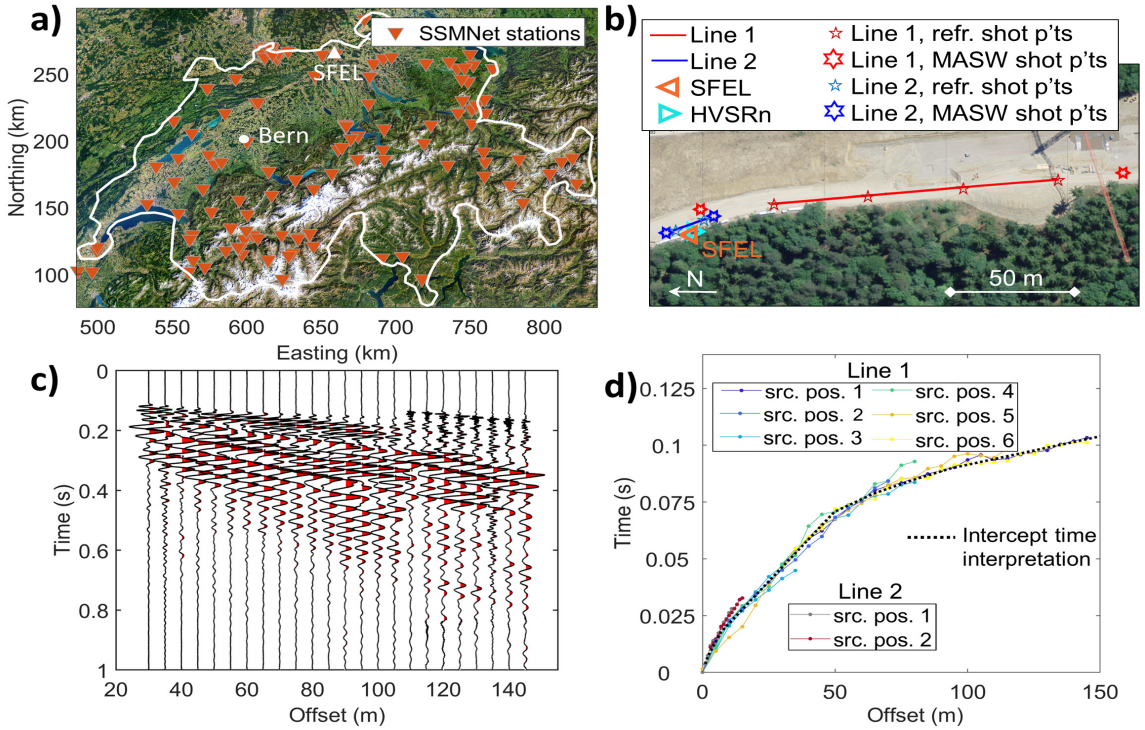

Fig. 1 – Site SFEL (Würenlingen, Switzerland). Seismic acquisition and P-wave refraction data interpretation. a) Map of the Swiss Strong Motion Network (SSMNet, updated September 2020) and location of station SFEL. b) Geometry of the data acquisition: location of the single-station microtremor recording for horizontal-to-vertical spectral ratio interpretation (HVSRn), location of the two geophone lines for active seismic measurement. c) vertical-component seismogram from line 1; the seismic source (weight-drop) is positioned north of the array. d) P-wave first-break arrivals from lines 1 and 2, represented in travel-time vs offset domain. Source positions are numbered, at both lines, progressing from north to south. The hodocrone from the intercept time interpretation is represented by the black dotted line.

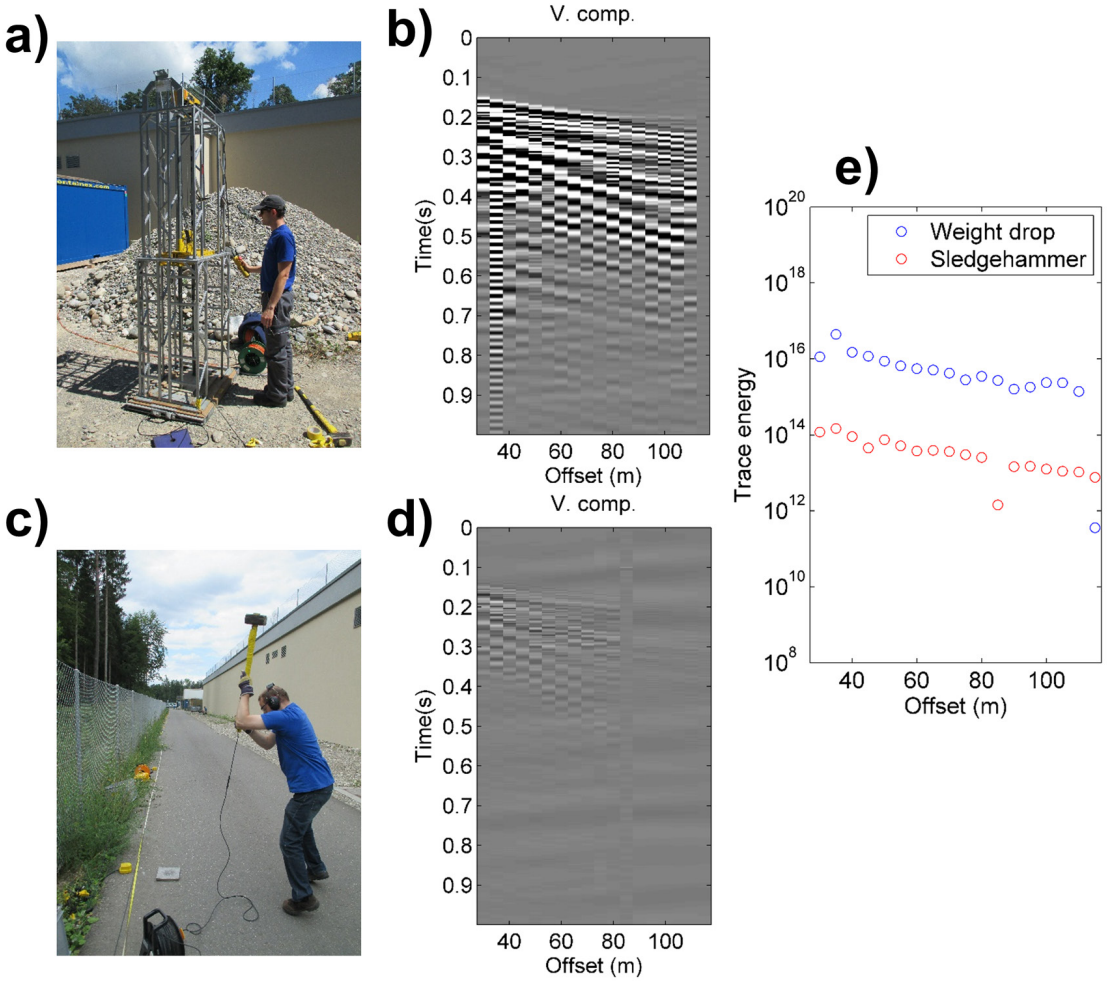

Fig. 2 – Comparison of the employed seismic sources (line 1). a) weight drop device; b) sample seismic section (vertical component) obtained with the use of the weight drop equipment; c) sledgehammer; d) sample seismic section (vertical component) obtained with the use of the sledgehammer as seismic source. Note that the color scale for the amplitudes is the same as in (b). e) energy (in arbitrary units) of the seismic traces shown in (b) and (d).

3. Data processing

The seismic sections from line 1 and 2, acquired for the observation of Rayleigh waves (i.e. with the seismic source positioned outside the geophone spread), were processed by means of both an *f-k* analysis (Socco and Strobbia, 2004, Foti et al. 2015) and the wavefield decomposition procedure introduced by Maranò et al (2017, implemented in the *WaveDecActive* code, https://stefanomarano.github.io/WaveDec/). While for the *f-k* analysis we inevitably interpreted separately the vertical- and radial-component traces, in the wavefield decomposition procedure the three recorded components are jointly processed, yielding a univocal description of Rayleigh wave propagation.

Fig. 3 shows the results of the surface wave processing from both active lines and processing techniques. The Rayleigh wave dispersion curves from *f-k* analysis (black and red continuous lines) were manually picked on the maxima of the stacked frequency-wavenumber spectra (Fig. 3a, Neducza, 2007); in Fig. 3b, these consistently draw a continuous dispersive branch spanning from 7 to 60 Hz with phase velocities decreasing from 1000 m/s down to 200 m/s. Faster phase velocity segments were also identified for frequencies > 15 Hz, although with a less coherent pattern.

The wavefield decomposition routine directly provides joint estimates of phase velocity, and ellipticity angle for each of the identified modal surface waves (Fig. 3b and 3c). Here again, a low-velocity branch extending from ~7 to 60 Hz is obtained; thanks to the attached information about the ellipticity and sense of particle motion (predominantly negative values of ellipticity angle, i.e. retrograde motion), this branch can be attributed to the fundamental mode of Rayleigh wave propagation (Foti et al., 2015; it is labelled with R0 in Figure 3b). At higher velocities, further wave estimates are available, grouping at f > 10-15 Hz into dispersive segments more coherent than their counterparts from *f-k* analysis; the clearest two were identified as first and second higher mode, respectively (labelled R1 and R2 in Figure 3b).

We highlight the fact that phase velocities and ellipticities from line 1 and 2 are generally in agreement in the overlapping wavenumber resolution band; in particular, the data from line 2 enable extending the fundamental mode information from 35 to 60 Hz.
The ellipticity angle information relevant to the identified fundamental mode, when translated into ellipticity (Fig. 3d), joins quite well with the Rayleigh ellipticity curve obtained from the single-station microtremor data processed with the RayDec algorithm (Hobiger et al. 2009), between 7 – 10 Hz. At higher frequencies the match is lost, as the RayDec curve becomes influenced by higher modes as well – in fact, in the same frequency range, higher modes clearly appear both in the *f-k* panel and in the wavefield decomposition estimates (Fig. 3a and b).
The target finally selected for the inversion is therefore constituted by the multimodal Rayleigh wave dispersion curve (modes from fundamental to 2nd higher), and by the fundamental mode ellipticity curve, both as obtained from the wavefield decomposition processing (Fig. 3b,c). At low frequency 7 Hz, the latter is joined to the ellipticity obtained from the single-station microtremor recording analysed with the RayDec technique (Hobiger et al., 2009), thus extending the target frequency band to 1 Hz (Fig. 3d), in order to constrain the deeper portion of the subsurface. The ellipticity peak between 3.5 and 5.5 Hz is removed from the target of the inversion, to allow for a possible singularity, as recommended by Hobiger et al. (2013).

The seismograms intended for seismic refraction analysis were processed by manually picking the first-break arrivals of P-waves on the vertical component traces. For line 1, considering the good signal-to-noise ratio obtained with the weight drop even at far offset, first-break arrivals were also picked on the seismograms primarily intended for surface wave analysis. The obtained hodocrones appear to describe a subsurface without significant lateral variations, as they approximately follow the same pattern, independently of the shooting position (Fig. 1d). Hence, they were collapsed into a single travel-time *vs* offset curve, interpreted with the intercept-time method (Reynolds, 2011); the resulting V_P profile is displayed in Fig. 4b, right panel.

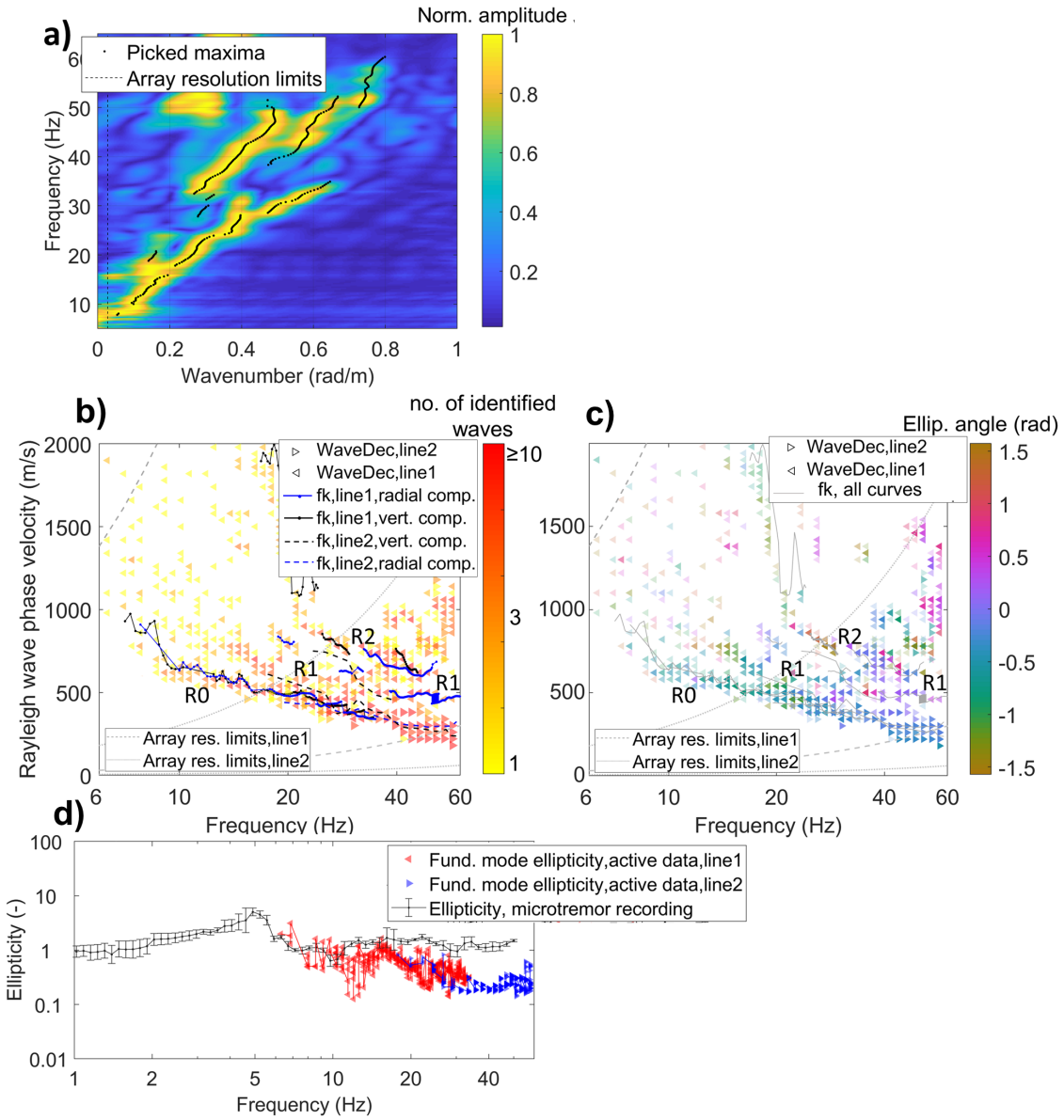

Fig. 3 - Site SFEL (Würenlingen, Switzerland). Rayleigh wave data processing and interpretation. a) Frequency-wavenumber panel derived from the vertical-component traces from line 1. Spectral amplitudes are normalized at each frequency. Picked energy maxima are represented as black dots. b) Collation between Rayleigh wave phase velocity estimates from f-k analysis and wavefield decomposition. f-k analysis: black and blue lines. Wavefield decomposition: triangles whose color represents the density of wave estimates (from all available shots) falling in the corresponding frequency-phase velocity bin. The labels R0 to R2 refer to the mode identification, from fundamental to second higher. c) Full representation of the wavefield decomposition processing results: joint Rayleigh wave velocity and ellipticity estimates. The color of the triangles represents the average ellipticity angle of the wave estimates falling in the corresponding frequency-velocity bin; the color intensity is proportional to the density of estimates. d) Ellipticity obtained from the processing of single-station microtremor data (black line), collated with the fundamental mode ellipticity from the active data processed with the wavefield decomposition technique (triangles).

4. Inversion

The experimental Rayleigh wave phase velocity and ellipticity curves, as obtained from wavefield decomposition processing, were jointly inverted for a V_S-V_P model of the subsurface. For the inversion, we implemented a Monte Carlo procedure, resorting to the codes of Hermann (2013) for the solution of the forward modelling. The subsurface was modelled as a stack of seven homogeneous layers overlying the halfspace. Thickness and S-wave velocity values are attributed to each layer with a random selection among pre-defined boundaries; the same holds for P-wave velocity values, provided that these are consistent with a realistic Poisson's ratio interval. Density values were assigned a priori to the various formations, increasing from 1800 kg/m^3 for the weathering layer to 2200 kg/m^3 for the halfspace. We simulated a total of 3 million different models, collating each time the theoretical curves with the experimental ones through the computation of the root mean square error (RMSE). In Fig. 4, we show the 30 best performing models, i.e. achieving the lowest RMSE. Fig. 4a shows the collation between the experimental curves and the synthetic ones, while we display the corresponding V_S and V_P velocity models in Fig. 4b.
We observe that all selected models achieve a RMSE lower than 1; also the visual comparison between experimental and simulated curves evidences a fairly good match (Fig. 4a). The corresponding S-wave velocity profiles (Fig. 4b, left panel) group into a relatively coherent description of the subsurface; in the shallowest 7.5 m (identified as weathering soil), V_S gradually increases from 250 to ~500 m/s. The depth range 7.5-18 m bears a V_S of about 550 m/s, and it can be attributed to the gravel terrace indicated by the local geological atlas (Swisstopo, 2006). Further below, between 18 – 45 m depth, S-wave velocity increases to approximately 850 m/s; this value is compatible with a layer of compact gravel with blocks and/or a compact moraine formation, as suggested by the geological profile of a well drilled 230 m south of SFEL. The water table is to be located at ~18 m depth, as both the V_P profile from refraction and the P-wave velocity models from Rayleigh wave data inversion exceed at that depth 1500 m/s; again, this finding is in agreement with the information from the aforementioned well and also coincides with the Aare's level located around 19 m below the investigated site (Fig. 4b). The (weathered) bedrock is probably met at 40-50 m depth, where V_S increments to about 1100 m/s; we remind that the 2D geological model of Swisstopo (2019) indicates a bedrock depth of circa 50 m in the investigated area. The stiffness of the fractured rock increases with depth, until reaching ~1750 m/s at 70 - 90 m depth. We also highlight the approximate agreement between the V_P profile obtained from refraction and the P-wave velocity models from Rayleigh wave data inversion, which are reciprocally independent estimates.
Finally, we compute the synthetic SH-wave transfer functions relative to the selected best-performing V_S models (Roesset, 1970). We then refer them to the Swiss standard rock model (Poggi et al., 2011), for direct comparison (Fig. 4c) with the experimental amplification function obtained at SFEL from the processing of recorded earthquake waveforms with the empirical spectral modelling technique (Edwards et al., 2013). The good match between simulated and empirical amplification functions indicates a purely 1D resonance pattern for the local response of the site.

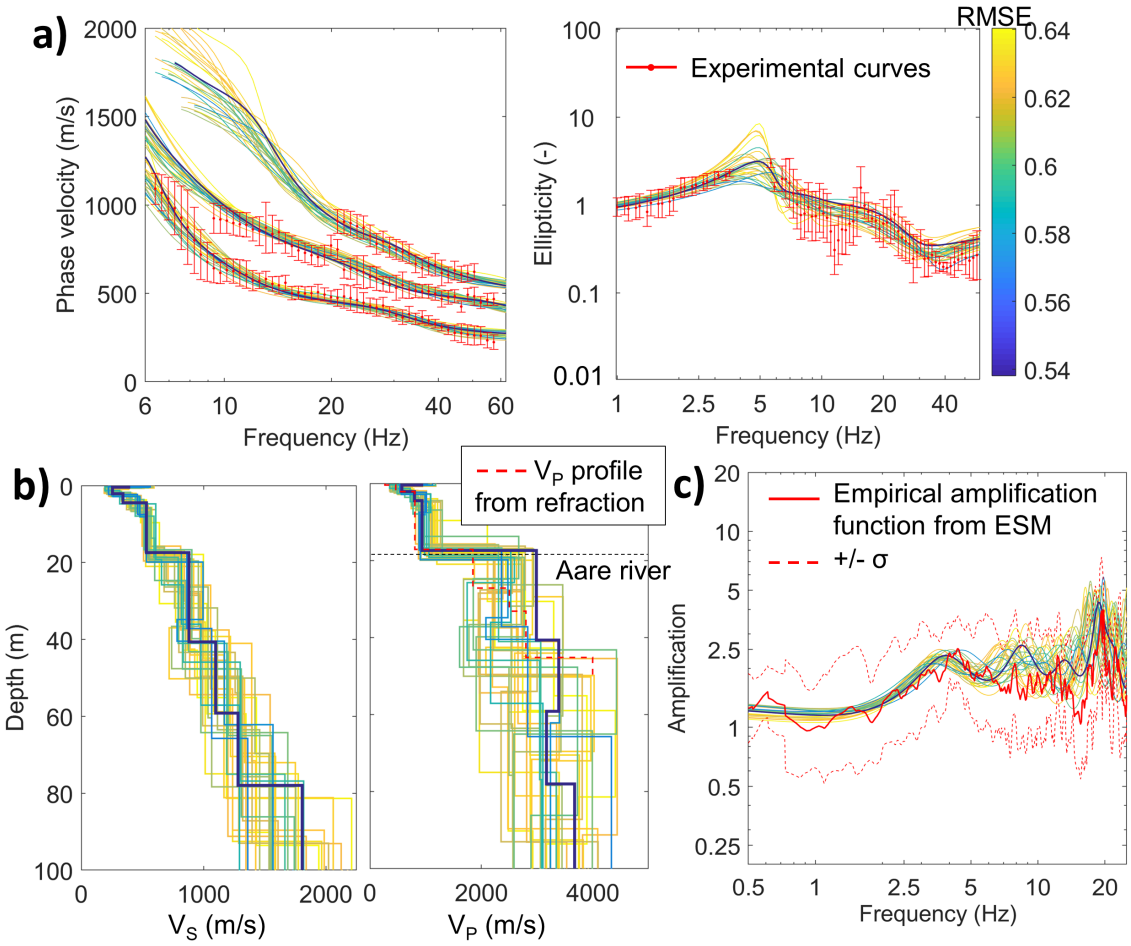

Figure 4 - Site SFEL (Wuerenlingen, Switzerland), Rayleigh wave data inversion results. a) Match between experimental phase velocity, ellipticity curves and the simulated curves from the 30 models achieving the lowest misfit (lines ranging from blue to yellow according to RMSE; the lowest misfit model is highlighted with a thicker line). b) Corresponding best performing V_S and V_P models. c) Comparison between simulated SH amplification functions from the V_S profiles in (b), referred to the Swiss standard rock profile, and the experimental amplification function determined for station SFEL from empirical spectral modelling.

4. Conclusion

We present a case study of the site characterization survey at a station of the Swiss strong motion network (SSMNet). The active seismic geophysical measurements were interpreted in terms of both Rayleigh-wave and P-wave refraction analysis. For the former, we processed the acquired data with a wavefield-decomposition approach leading to the estimation of multi-modal Rayleigh wave dispersion and ellipticity curves. The joint inversion of these curves produced a Vs model of the subsurface well constrained over a wide depth range. The V_P model obtained from the refraction survey enabled to exclude the presence of relevant lateral variations. The synthetic SH-transfer function derived from the obtained Vs profile well matches the empirical amplification function retrieved by interpreting earthquake recordings at the station with the empirical spectral modelling technique. The match indicates a purely 1D resonance pattern for the local response of the station's site. As conclusion of the study, we argue that a thorough, multi-method geophysical surveying can play key role in characterizing the local seismic site response and determining whether 2-3D resonance effects are present or not.

Acknowledgements

The renewal project of the Swiss strong-motion network was financed by the Federal Office of the Environment (FOEN) of Switzerland. Special thanks go to Blaise Duvernay for his continuous support of the project. We also thank Armin Ziegler, Ziegler Consultants, for providing the weight drop device

References

- Bergamo P. et al., (2016). SITE CHARACTERIZATION REPORT SFEL: Paul Scherrer Institut (AG), SwissFEL. Swiss Seismological Service (SED) at ETH Zurich.
- Edwards, B., et al. (2013). Determination of Site Amplification from Regional Seismicity: Application to the Swiss National Seismic Networks, Seismological Research Letters, 84(4), 611-621.
- Foti, S., et al. (2011). Application of Surface-Wave Methods for Seismic Site Characterization, Surveys in Geophysics, 32, 777-825.
- Foti, S., et al. (2015). Surface wave methods for near-surface site characterization, pp. 96 – 120, 255 – 272, CRC Press, Taylor & Francis Group LLC
- Garofalo, F., et al., (2016a). InterPACIFIC project: Comparison of invasive and non-invasive methods for seismic site characterization. Part I: Intra-comparison of surface wave methods, Soil Dynamics and Earthquake Engineering, 82, 222-240.
- Garofalo, F. et al., (2016b). InterPACIFIC project: Comparison of invasive and non-invasive methods for seismic site characterization. Part II: Inter-comparison between surface-wave and borehole methods. Soil Dynamics and Earthquake Engineering 82, 241-254.
- Herrmann, R. B. (2013) Computer programs in seismology: An evolving tool for instruction and research, Seism. Res. Lettr. 84, 1081-1088, doi:10.1785/0220110096
- Hobiger, M., et al., (2009). Single station determination of Rayleigh wave ellipticity by using the random decrement technique (RayDec). GRL, 36, L14303.
- Hobiger, M., et al., (2013). Ground structure imaging by inversion of Rayleigh wave ellipticity: sensitivity analysis and application to European strong motion sites. GJI, 192, 207-229
- Hobiger, M. et al. (2021). Site Characterization of Swiss Strong-Motion Stations: The Benefit of Advanced Processing Algorithms, Bulletin of the Seismological Society of America, 111:4, 1713–1739
- Hollender, F., et al. (2018). Characterization of site conditions (soil class, VS30, velocity profiles) for 33 stations from the French permanent accelerometric network (RAP) using surface-wave methods, Bull. Earthquake Eng., 16, 2337–2365.
- Kaiser, A., et al., (2017). Site characterization of GeoNet stations for the New Zealand strong motion database, Bulletin of the New Zealand Society for Earthquake Engineering 50, 39–49.
- Kaklamanos, J. & Bradley, B. A., 2018. Challenges in predicting seismic site response with 1D analyses: conclusions from 114 KiK-net vertical seismometer arrays, Bull. seism. Soc. Am., 108(5A), 2816–2838
- Laurendeau, A. et al., (2018). Derivation of consistent hard rock (1000 < VS < 3000 m/s) GMPEs from surface and down-hole recordings: Analysis of KiK-net data, Bulletin of Earthquake Engineering 16, 2253–2284.
- Maranò, S., et al., (2012). Seismic waves estimation and wavefield decomposition: application to ambient vibrations, Geophys. J. Int., 191:1, 175–188
- Maranò, S., et al. (2017). Analysis of Rayleigh waves with circular wavefront: a maximum likelihood approach, Geophys. J. Int., 210:3, 1570–1581
- McMechan, G. A., & Yedlin, M. J. (1981). Analysis of dispersive waves by wave field transformation. Geophysics, 46(6), 869-874.
- Michel., C. et al., (2014) Assessment of Site Effects in Alpine Regions through Systematic Site Characterization of Seismic Stations. Bulletin of the Seismological Society of America; 104 (6): 2809–2826. doi:10.1785/0120140097
- Nakamura Y., (1989). A method for dynamic characteristics estimation of subsurface using microtremor on the ground surface. Quaterly Report Railway Tech. Res. Inst., 30-1, 25- 30.
- Neducza, B., (2007), Stacking of surface waves: Geophysics, 72, 51–58.
- Park C.B., et al., (1999). Multichannel analysis of surface waves. Geophysics 64, 800–808.

- Poggi, V., Edwards, B., and Fäh, D. (2011). Derivation of a Reference Shear-Wave Velocity Model from Empirical Site Amplification. Bulletin of the Seismological Society of America, 101(1):258–274.
- Redpath, B. B., (1973). Seismic refraction exploration for engineering site investigations: National Technical Information Service, Technical Report E-73-4.
- Reynolds, J.M., (2011). An introduction to applied and Environmental Geophysics: John Wiley& Sons, Ltd.
- Roesset, J. (1970). Fundamentals of soil amplification. In Hansen, R. J., editor, Seismic Design for Nuclear Power Plants, pages 183–244. M.I.T. Press, Cambridge, Mass.
- Socco, L.V. and C. Strobbia (2004). Surface-wave method for near-surface characterization: a
- tutorial. Near Surface Geophysics, 2004, 165-185.
- Swiss Federal Office for Topography, Swisstopo, 2006. 1:25000 Geological Atlas, sheet 120 Baden (LK1070).
- Swisstopo, Swiss Federal Office of Topography (2019). Grossezza da la crappa lucca da la Svizra, https://www.swisstopo.admin.ch/it/geodata/geology/models/unconsolidated-deposits.html
- Tao, Y. & Rathje, E., (2020). Taxonomy for evaluating the site-specific applicability of one-dimensional ground response analysis, Soil Dyn. Earthq. Eng., 128, 105865
- Xia, J., Xu, Y., & Miller, R. D. (2007). Generating an image of dispersive energy by frequency decomposition and slant stacking. Pure and Applied Geophysics, 164(5), 941-956
- Yong, A., Martin, A., Stokoe, K. & Diehl, J., (2013). ARRA-funded VS30 measurements using multi-technique approach at strong-motion stations in California and central-eastern United States, U.S. Geological Survey Open-File Report 2013-1102.
- Zywicki, D. J. (1999). Advanced signal processing methods applied to engineering analysis of seismic surface waves (Doctoral dissertation, Georgia Institute of Technology).